AJNR

MR Imaging Quantification of Cerebellar Growth Following Hypoxic-Ischemic Injury to the Neonatal Brain

Elisabeth Le Strange, Nadeem Saeed, Frances M. Cowan, A. David Edwards and Mary A. Rutherford

AJNR Am J Neuroradiol 2004, 25 (3) 463-468
http://www.ajnr.org/content/25/3/463

AJNR Am J Neuroradiol 25:463–468, March 2004

MR Imaging Quantification of Cerebellar Growth Following Hypoxic-Ischemic Injury to the Neonatal Brain

Elisabeth Le Strange, Nadeem Saeed, Frances M. Cowan,
A. David Edwards, and Mary A. Rutherford

BACKGROUND AND PURPOSE: **Cerebellar atrophy may occur as a result of a primary injury, such as infarction or hemorrhage. Impaired growth of a noninjured cerebellum may be seen as a secondary effect related to damage in other remote but connected areas of the brain, or so-called diaschisis. We sought to determine whether perinatal hypoxic-ischemic injury leads to poor cerebellar growth and whether such impairment occurs asymmetrically in infants with predominantly unilateral brain injury.**

METHODS: **We used a computerized quantification program to measure cerebellar size by using serial MR images. Term-born infants presenting with encephalopathy and/or seizures presumed due to a hypoxic-ischemic insult within 48 hours of delivery were included if they had two or more volume acquisition images obtained at least 3 months apart but within the first 15 months of delivery.**

RESULTS: **When data were grouped by MR appearances, significant differences in total cerebellum growth were seen between infants with focal infarction and those with basal ganglia and thalamic injury ($P < .001$). Unilateral forebrain lesions shown on MR imaging were not predictive of asymmetric cerebellar growth.**

CONCLUSION: **Infants with focal infarction of the cerebral hemisphere had an apparently normal pattern of growth in both cerebellar hemispheres. However, in infants with severe basal ganglia and thalamic lesions, cerebellar growth was reduced, and the vermis showed little or no growth during the first year after birth.**

MR imaging can depict abnormalities of the neonatal cerebellum, such as congenital cerebellar hypoplasia or acquired atrophy. In the older child and adult brain, the most common causes of cerebellar atrophy are heritable and degenerative disorders, whereas in the neonate, atrophy may follow perinatally acquired hemorrhagic or ischemic lesions (1). In addition, poor growth of the cerebellum may occur as a secondary effect related to damage in other remote but connected areas of the neonatal brain (2), or so-called diaschisis (3). The cerebellum is increasingly recognized as an important component of the brain in functions other than motor control (4). As a result, it has become important to find objective ways to assess the cerebellum in various disease states and after injury. As visual analysis of the cerebellum by imaging is difficult, determination of cerebellar volume may prove useful in such assessments.

Manual methods of cerebellar isolation from MR images are subjective and time consuming. Aids to manual outlining of the cerebellum include thresholding (5) and more-complicated algorithmic attempts to determine boundaries (6). In a novel technique, the brain is mapped to a standard coordinate system and regions of interest are determined from a detailed atlas (7). However, adaptation of such an atlas to the rapidly growing infant brain presents considerable difficulties. We have developed a computerized quantification program for measuring cerebellar size on MR images in the immature brain (8, 9).

We used a computerized quantification program to measure cerebellar size on serial MR images in term infants with evidence of perinatal hypoxic-ischemic brain injury but without visible damage in the cerebellum on conventional MR imaging. The aim was to

Received March 25, 2003; accepted August 26.

From the Robert Steiner Magnetic Resonance Unit, Imaging Sciences Department (E.L.S., N.S., M.A.R.) and the Department of Pediatrics and Neonatal Medicine (F.M.C., A.D.E., M.A.R.), Imperial College, Hammersmith Campus, London, England.

Dr Rutherford is supported by the Medical Research Council.

Author reprint requests to Mary Rutherford, Robert Steiner MRI Unit, Imaging Sciences Department, Imperial College, Hammersmith Campus, Du Cane Road, London W12 OHS, England.

Clinical details and timing of studies

Patient no.	Gestation	Fetal Distress*	Delivery†	Apgar Scores	Birthweight, kg	MR Imaging Findings‡	Age at Studies	Outcome	Head Circumference at ≥12 mo
1	41	Ctg/msl	Nvd	5,8	3.75	Transient bg	2 d, 3 d, 4 m	Normal	1st
2	40	Ctg	Emcd	1,7	2.46	Normal	3 m, 6 m	Normal	25th
3	40	Ctg	Emcd	1,5	3.12	Transient bg	6 d, 1 m, 3 m, 7 m	Normal	50th
4	41	Nil	Nvd	7,9	3.56	Infarct, left	1 m, 2 m	Normal	25th
5	39	Nil	Nvd	3,5	3.35	Infarct, left	1 m, 3 m, 5 m	Moderate	<0.4th
6	40	Nil	Nvd	9,10	2.84	Infarct, left	1 m, 3 m, 8 m	Normal	75th
7	40	Ctg	Emcd	2,7	3.68	Infarct, left	2 d, 3 d, 9 d	Normal	9–25th
8	41	Ctg/msl	Emcd	5,9	2.9	Infarct, right	2 d, 9 d, 1 m, 3 m, 6 m	Normal	2–9th
9	41	Msl	Emcs	4,9	3.12	Infarct, right	3 m, 5 m, 9 m	Moderate	25th
10	41	Ctg/msl	Forceps	5,7	4.25	Infarct, left	6 d, 1.5 m, 3 m, 6 m	Normal	25th
11	42	Msl	Ventouse	6,8	3.1	Infarct, left	6 d, 1 m, 3 m	Normal	25th
12	39	Nil	Nvd	7,10	3.59	Infarct, left	6 m, 21 m	Moderate	91st
13	39	Nil	Nvd	5,7	3.34	Infarct, left	7 d, 1 m, 3 m, 8 m	Normal	<25th
14	41	Ctg/msl	Emcd	2,8	3.22	Infarct, left	9 d, 16 d, 1.5 m, 3 m, 6 m	Moderate	20th
15	42	Ctg	Emcd	0	NA	Severe bg	1.3 m, 3.5 m, 12 m	Severe	<3rd
16	41	Ctg	Forceps	1,4	2.8	Severe bg, wm	1.5 m, 6 m	Severe	<0.4th
17	42	Ctg/msl	Forceps	0,0	4	Severe bg	11 m, 14 m	Severe	<0.4th
28	39	Ctg/msl	Emcd	0,0	3.08	Severe bg	11 d, 2 m, 6.5 m, 12 m	Severe	<0.4th
19	40	Ctg	Nvd	0,3	3.13	Moderate bg	14 d, 4.5 m, 11.5 m	Severe	45th
20	40	Ctg	Nvd	5,7	3.98	Severe bg	6 m, 13.5 m	Severe	<0.4th

* Ctg indicates cardiotocograph; msl, meconium-stained liquor.

† Emcd indicates emergency cesarean delivery; nvd, normal vaginal delivery.

‡ bg indicates basal ganglia lesions; wm, white matter.

determine if perinatal hypoxic-ischemic injury leads to impaired cerebellar growth and if impaired growth occurs asymmetrically in infants with predominantly unilateral brain injury. We hypothesized that cerebellar growth is impaired as a secondary phenomenon following unilateral or bilateral perinatal injury to the supratentorial brain structures.

Methods

Patients

This study was approved by the hospital ethics committee. Parental consent was obtained for each scan. Term-born infants (greater than 37 weeks' gestation) presenting with an encephalopathy and/or seizures presumed due to a hypoxic-ischemic insult within 48 hours of delivery were included. Infants with an encephalopathy had signs of fetal distress and low Apgar scores of less than 5 at 5 minutes. All initial imaging abnormalities were consistent with an acute injury to the brain (10). Infants with congenital malformations, preexisting antenatally acquired lesions, evidence of acquired or congenital infection, or metabolic disease or visual abnormalities within the cerebellum were excluded. Infants were included if they had two or more volume acquisition images to enable the assessment of cerebellar size and growth over at least a 3-month period. Results from birth to 15 months of age were included in this study. Clinical details of the infants and the timing of their MR studies are shown in Table 1.

Control Subjects

For the purposes of this study, infants with normal appearances on initial imaging or transient mild brain swelling with no persisting abnormality and those who had normal neurodevelopmental outcomes were used as control subjects.

Neurodevelopment Outcome

All the infants were examined at regular intervals for clinical assessment. All underwent an evaluation of neurodevelopmental progress with the Griffiths developmental assessment (11) and standardized neurologic examination at 1 year of age (12). Head circumferences were measured at each follow-up examination and plotted on the centile charts (13). Infants with abnormal neurologic findings were defined as having a hemiplegia, diplegia, or quadriplegia. Infants with a hemiplegia were classified as having a moderate outcome, and those with diplegia or quadriplegia were classified as having a severe outcome. Infants without an abnormal tone outcome were classified according to the Griffths score. An abnormal outcome included a development quotient (DQ) < 85. These abnormal outcomes were subdivided as mild (DQ, 75–84), moderate (DQ, 50–74), or severe (DQ <50).

Image Acquisition

All images were obtained by using a Picker 1 T HPQ magnet (Cleveland, OH). All infants were examined with conventional T1- and T2-weighted spin-echo and age-related inversion recovery sequences in the transverse plane. T1-weighted, 3-dimensional, RF spoiled, volume images were obtained in the sagittal plane (TR/TE/NEX, 21/6/2; flip angle, 35°; FOV, 25 cm; matrix, 152×256; 114 sections). The section thickness was 1.6 mm, and in-plane resolution was 0.98×0.98 mm. The timing of these studies is shown in Table 1.

Image Analysis

The conventional T1- and T2-weighted images were used to assess the presence of normal anatomy and to identify sites of injury. Infants were grouped according to the pattern of their injury. Group I ($n = 3$) included infants with no persistent lesions on imaging. These infants, who had normal neurodevelopment at follow-up, were used as control subjects. Group 1I ($n = 11$) included infants with focal unilateral infarction (Fig 1A) (nine left sided and two right sided). One infant in this

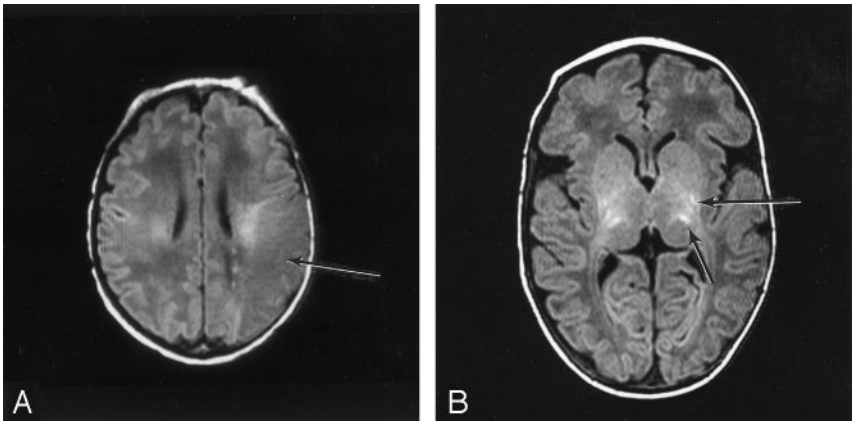

FIG 1. T1-weighted MR images (860/20).
A, Day 5 image shows focal infarction. There is a loss of gray matter–white matter differentiation in the posterior lobe on the left. This is consistent with perinatal infarction within the territory of the left middle cerebral artery.
B, Day 12 image shows basal ganglia and thalamic lesions. There are persistent, abnormal high-signal-intensity regions in the posterior lentiform nuclei and lateral thalami (*arrows*). The intervening posterior limb of the internal capsule shows reduced high signal intensity from myelin.

group only had one volume acquisition within the time period studied. Group III ($n = 6$) included infants with persistent bilateral basal ganglia and thalamic lesions with abnormal signal intensity within the posterior limb of the internal capsule (Fig 1B) (14). These infants may also have shown associated abnormalities in the cortex and white matter. The white matter changes may have been obvious on the first scan (Table 1), or they developed subsequently as a result of atrophy.

Cerebellar Quantification

The cerebellum was quantified by using the T1-weighted volume acquisition images. The operator installed an initial contour that surrounded the cerebellum within a central section. This was then manually edited, predominantly by removing pixels determined not to be cerebellum, to obtain a closely matching contour. The contour encompassed both the gray matter and white matter. The peduncles were excluded. The contour was replicated on an adjacent section and edited in the same fashion. Except for a few central sections, the shape of the cerebellar hemispheres varied slowly. With this method, installing contours for every section that contained cerebellar tissue was not unduly time consuming.

The volume of the cerebellum was determined by multiplying the total voxel area within the contours by the section thickness. As previously stated, the peduncles were not included, and the central midline section was assessed with reference to the appearance of the vermis. A measure of vermal surface area was also made by isolating the contour, which gave the maximum cross-sectional area for the vermis. This was chosen with reference to the standard appearance of the vermis, by removing any parts of the tonsil and hemispheres visible in the midline sections. The following volumes were obtained for each set of images: left cerebellar hemisphere, right cerebellar hemisphere, total cerebellar volume, and maximal vermal area.

The intraobserver and interobserver (M.A.R., E.L.S.) errors for measurements of cerebellar volume were estimated to be within 2% and 4%, respectively (95% confidence interval).

Statistical Analysis

Data were tested for normality by using the Shapiro-Wilkes test before each analysis and transformed when appropriate. A normal distribution of residuals was confirmed. The relations of both total cerebellar volume and vermal area to age in each outcome group and in each MR imaging group were determined. The rate of change in tissue volume with respect to time was then calculated and compared between outcome groups by means of one-way analysis of variance with the Bonferroni multiple comparison test.

Cerebellar volumes ipsilateral and contralateral to any unilateral lesion were also compared in infants with and those without forebrain lesions. To analyze this, the hemicerebellar to total cerebellar volume ratio (HCVR) was calculated. In infants with unilateral lesions, the volume of the hemicerebellum ipsilateral to the forebrain lesions were calculated, and in infants without forebrain lesions, the volume of the right hemicerebellum was used to create a control variable. The null hypothesis of the analysis stated that growth is equal on both sides of the cerebellum, and therefore, the mean HCVR in each group is not significantly different from 0.5. The mean HCVR was calculated for each MR imaging and outcome group.

Results

A total of 62 volume acquisition images were quantified for the 20 infants. The clinical details and neonatal imaging findings are shown in Table 1. The final imaging studies were performed at a median of 6 months (range, 2–9 months) in the infarct group and a median of 11 months (range, 4–14 months) in the hypoxic-ischemic encephalopathy group.

Total Cerebellar Growth

During the first 4 weeks after birth, the median total cerebellar volume was 23.52 cm^3 (range, 19.63–32.78), reaching values of 100 cm^3 by the end of the first year. The rate of change of total cerebellar volume was normalized by inverse square root transformation. Univariate analysis showed that, for total cerebellar volume, there was a significant linear relation between tissue volume and age, both overall and when the data were divided into subgroups by either outcome or MR appearances ($P < .005$) (Fig 2). These tests showed that it was appropriate to calculate the rate of change of tissue volume with respect to age and to compare the values of the subgroups. This analysis showed that, when data were grouped by MR appearances, significant differences in total cerebellum growth were seen between groups II and III ($P < .001$). However, differences between groups I and III did not reach conventional statistical significance ($P = .11$ for total cerebellum volume and $P = .065$ for vermal area).

Analysis of the effect of unilateral forebrain lesions on cerebellar growth showed that, in each MR imaging group, the HCVR was not significantly different from 0.5. Thus, unilateral forebrain lesions on MR

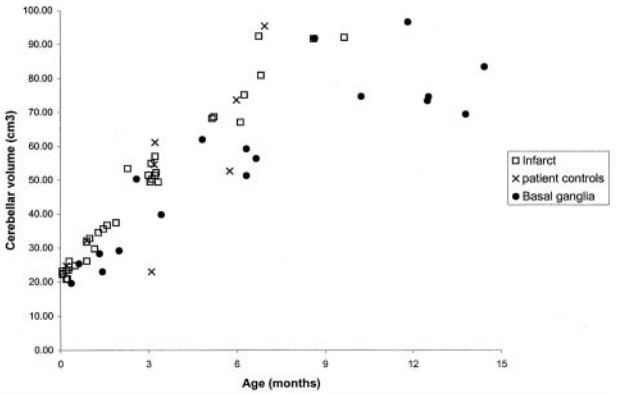

FIG 2. Total cerebellar volume versus age in all infants, by group ($n = 20$).

imaging were not predictive of asymmetric cerebellar growth (Figs 3, 4).

Vermal Growth

Univariate analysis showed that, for the vermis, there was a significant linear relation between vermal area and age, both overall and when the data were divided into subgroups by outcome or MR appearance ($P < .005$) (Fig 5). The rate of change in vermis area required log-skew transformation according to the form $x = \ln(y - 30.140)$ where x is the transformed value and y is the raw data. Infants in group III had little vermal growth, significantly different to the other groups ($P < .05$). In groups I and II, vermal growth was proportional to total cerebellar growth, but in group III, the vermis grew relatively less than did the cerebellar hemispheres (Fig 6).

Cerebellar Growth and Neurodevelopmental Outcome

When the infants were subgrouped according to outcome, there were significant differences in the rate of change over time in the vermal area and in total cerebellar volumes between the normal and severe ($P < .001$) and the mild and severe ($P < .02$) outcome groups. In all analyses, the rate of growth was lower in those with a severe outcome.

Head Circumference

In infants whose head circumference was abnormal at 12 months of age (less than the third percentile), both total cerebellar volume and vermal area were

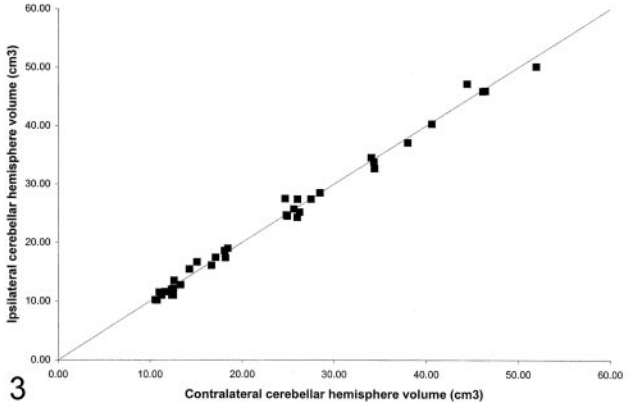

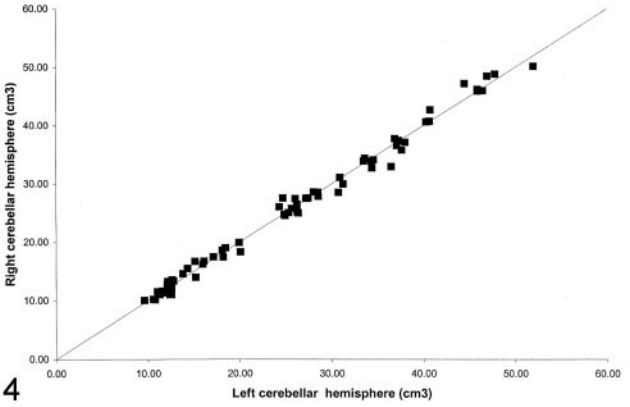

FIG 3. Cerebellar hemispheres in infants with cerebral infarcts. Volume ipsilateral to the infarct versus volume contralateral to the infarct ($n = 11$). The line is the line of equality.

FIG 4. Cerebellar hemispheres in all infants. Volume of the right hemisphere versus volume of the left hemisphere ($n = 20$). The line is the line of equality.

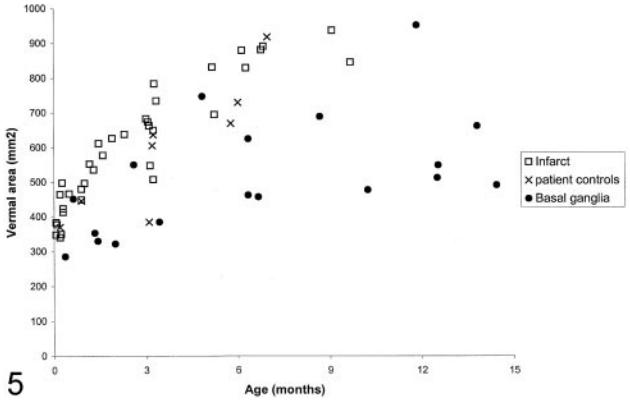

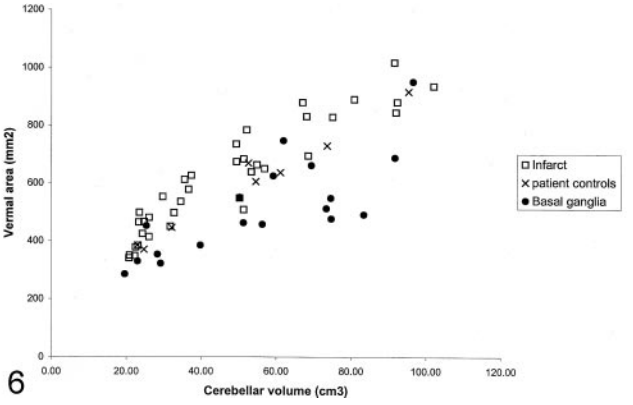

FIG 5. Cross-sectional area of the vermis versus age ($n = 20$).

FIG 6. Cross-sectional area of the vermis versus total cerebellar volume ($n = 23$).

significantly smaller than those in infants with a head circumference within the normal range.

Discussion

We have used a reliable quantifiable method for measuring the infant cerebellum and have shown that, in most children examined, the cerebellum and vermis grew in a linear fashion during the first year after term birth, even in children with normal images appearances and outcomes. This finding is in contrast to the rate of growth of the head and cerebral hemispheres, which gradually decreases over this same period. The neonatal cerebellum weighs approximately 18–20 g, or only 5%–6% of the brain weight (15), compared with 10% in the adult. Cerebellar development is known to continue after birth, with continuing cell differentiation and migration.

Infants with focal infarction of the cerebral hemisphere had an apparently normal pattern of growth in both cerebellar hemispheres within the period studied. However, in infants with severe basal ganglia and thalamic lesions, cerebellar growth was linear but reduced in comparison to the other two groups, and the vermis showed virtually no growth over the first year after birth. We were unable to find a difference in total cerebellar growth between the control subjects and those with severe basal ganglia lesions, but this was probably a type II effect due to the small number of control subjects, a weakness of this study. We did not have permission to perform serial imaging in healthy control infants, as this would have involved sedation for imaging performed outside the neonatal period. We therefore had to rely on a few patients who underwent serial imaging but who have had normal images and normal developmental follow-up to date. We appreciate the fact that cognitive effects of poor cerebellar growth may not be apparent until children are in the school system and that, ideally, follow-up should be for at least 6 years.

The method used to assess the cerebellum for this study was time consuming, but less so with repetition. It took up to 3 hours to perform one set of cerebellar hemisphere and vermis measurements. Specific protocols made reproducibility easier to achieve and consistent results obtainable, even on images of poor quality. These features make it more useful than more automated methods, which usually require ideal-quality images to work effectively. Serial imaging of adults often involves precise positioning to aid comparisons between studies; this is harder to achieve in infants, and its value is less clear, as growth makes direct comparisons impossible.

We were unable to find information on the absolute values for cerebellar weight or volume in the developing infant. Postmortem, the cerebellum is usually weighed with the rest of the brain. We therefore do not have a criterion standard for absolute or relative cerebellar growth in this age group, though some measures of fetal cerebellar growth have been obtained by using antenatal sonography (16).

Studies using positron emission tomography (PET) and single photon emission CT (SPECT) in adult stroke have detected hypometabolism in the cerebellum, the most common pattern being crossed cerebellar diaschisis in which the cerebellum is affected contralateral to a cerebral lesion (17, 18). Animal experiments have shown increased apoptosis in the cerebellum following forebrain injury (19). In adult patients with partial epilepsy and cortical foci, both contralateral diaschisis and cerebellar atrophy have been noted, and in adults with hemispheric cortical lesions following stroke, morphologic cerebellar atrophy matching the degree of atrophy in the contralateral cortex has been reported (3, 18, 20, 21). In our study, the symmetry of the cerebellar hemispheres in infants with unilateral infarcts suggests that any diaschisis that may occur acutely was not sufficient to cause reduced growth during infancy.

The infant brain has great plasticity, as shown by its regrowth after perinatal infarcts (22) and by the presence of presumed hypertrophy of ipsilateral tracts (23). Compensatory processes may ensure that the cerebellum maintains sufficient functioning connections to promote normal growth. However, most of these data come from the infant born at full term, and the maturational age of the brain at the time of injury may influence these processes. There are reported cases of cerebellar atrophy in association with focal forebrain lesions; these are mainly in preterm infants. However, many of these cases may have resulted from a primary lesion in the cerebellum.

We have demonstrated relative cerebellar atrophy in infants with severe basal ganglia lesions, although this was not obvious on visual analysis of the images. These infants have had substantial global insults; lesions in the basal ganglia are early markers by which the damage can be recognized. Other visible sites of injury include the cortex and subcortical white matter (24). In contrast, the cerebellum usually had a normal appearance on the conventional neonatal MR images. In addition, there was no evidence to support a congenitally small cerebellum in these infants. Primary cerebellar injury in infants with severe injury may not be obvious on early MR imaging (25), but in a group of 75 term infants with perinatal encephalopathy and/or seizures, we were unable to detect any changes in the cerebellum with diffusion-weighted imaging (M. A. Rutherford, unpublished data, 2003). It is possible, therefore, to postulate that connections from the basal ganglia to the cerebellum mediate the cerebellar abnormalities noted.

It would be of interest to compare the cerebellar measurements with a whole-brain volume measurement, but this was beyond the scope of this study. We used a simple measurement of overall head growth in the form of the head circumference centile as a surrogate measure of brain growth. None of the infants with a normal head circumference had a widened extracerebral space or dilatation of the ventricles. We therefore believed that head circumference was an acceptable marker for total brain size. Although the numbers are small, in infants with poor head growth in association with basal ganglia and thalamic lesions,

there was cerebellar atrophy. Infants with severe basal ganglia lesions may have secondary microcephaly out of proportion to the amount of initial damage; this is assumed to reflect a secondary effect on the developing white matter (26). A similar process may result in secondary cerebellar atrophy.

Infants with clinically important basal ganglia and thalamic damage had almost no growth of the cerebellar vermis. Damage to specific cerebellar nuclei in combination with basal ganglia and thalamic damage may possibly cause atrophy of fibers traversing the vermis. One infant in group III had relative preservation of the vermis and less severe growth retardation of both head circumference and cerebellar volume. The initial MR images depicted moderate basal ganglia changes rather than the severe changes of others in this group.

Further detailed examination of basal ganglia lesions may reveal specific sites of damage that could be more directly responsible for cerebellar changes. Successive projections occur from the lateral cerebellar hemispheres to the dentate nuclei, the ventrolateral thalamic nucleus, and the precentral gyrus (27). However, the ventrolateral nuclei of the thalami, which are primary relay stations to the cerebellum, were abnormal on MR imaging in the infant with only moderate basal ganglia and thalamic changes and with good cerebellar and vermal growth.

This study demonstrates the role of quantification in MR imaging in understanding the response of the immature brain following perinatal hypoxic-ischemic injury.

Acknowledgments

We wish to thank the Medical Research Council and the Weston Foundation.

References

1. Mercuri E, He J, Curati WL, Dubowitz LMS, Cowan FM, Bydder GM. **Cerebellar infarction and atrophy in infants and children with a history of premature birth.** *Pediatr Radiol* 1997;27:139–143
2. Rollins NK, Wen TS, Dominguez R. **Crossed cerebellar atrophy in children: a neurologic sequela of extreme prematurity.** *Pediatr Radiol* 1995;25(Suppl 1):S20–S25
3. Bohnen NI, O'Brien TJ, Mullan BP, So EL. **Cerebellar changes in partial seizures: clinical correlations of quantitative SPECT and MRI analysis.** *Epilepsia* 1998;39:640–650
4. Allin M, Matsumoto H, Santhouse A, et al. **Cognitive and motor function and the size of the cerebellum in adolescents born very preterm.** *Brain* 2001;124:60–66
5. Luef G, Burtscher J, Kremser C, et al. **Magnetic resonance volumetry of the cerebellum in epileptic patients after phenytoin overdosages.** *Eur Neurol* 1996;36:273–277
6. Luft AR, Skalej M, Welte D, et al. **A new semiautomated, three-dimensional technique allowing precise quantification of total and regional cerebellar volume using MRI.** *Magn Reson Med* 1998;40:143–151
7. Andreasen NC, Rajarethinam R, Cizadlo T, et al. **Automatic atlas-based volume estimation of human brain regions from MR images.** *J Comput Assist Tomogr* 1996;20:98–106
8. Saeed N, Le Strange ET, Rutherford M, Puri BK. **Cerebellum segmentation employing texture analysis and knowledge based image processing.** Berkeley: International Society for Magnetic Resonance in Medicine, 1999:abstract 2190
9. Saeed N, Puri BK. **Cerebellum segmentation employing texture properties and knowledge based image processing: applied to normal adult controls and patients.** *Magn Reson Imaging* 2002;20:425–429
10. Cowan F, Rutherford M, Groenendaal F, et al. **Origin and timing of brain lesions in term infants with neonatal encephalopathy.** *Lancet* 2003;361:736–742
11. Griffiths R. *Infant Scales: Birth to Second Birthday (Revised)—Association for Research in Infant and Child Development.* Henley, UK: The Test Agency Ltd. 1996.
12. Haataja L, Mercuri E, Regev R, et al. **Optimality score for the neurologic examination of the infant at 12 and 18 months of age.** *J Pediatr* 1999;135:153–161
13. *Boys/Girls Four-in-One Growth Charts (Birth-20 Years): United Kingdom Cross-Sectional Reference Data: 1996/1.* Child Growth Foundation. *Prenat Diagn. Wiley Interscience* 1996
14. Rutherford MA, Pennock JM, Counsell SJ, et al. **Abnormal magnetic resonance signal in the internal capsule predicts poor neurodevelopmental outcome in infants with hypoxic-ischemic encephalopathy.** *Pediatrics* 1998;102:323–328
15. Crelin EA. *Functional Anatomy of the Newborn.* London: Yale University Press. 1973
16. Malinger G, Ginath S, Lerman-Sagie T, Watemberg N, Lev D, Glezerman M. **The fetal cerebellar vermis: normal development as shown by transvaginal ultrasound.** *Prenat Diagn* 2001;21:687–692
17. Nuutinen J, Kuikka J, Roivainen R, Vanninen E, Sivenius J. **Early serial SPET in acute middle cerebral artery infarction.** *Nucl Med Commun* 2000;21:425–429
18. Komaba Y, Osono E, Kitamura S, Katayama Y. **Crossed cerebellocerebral diaschisis in patients with cerebellar stroke.** *Acta Neurol Scand* 2000;101:8–12
19. Joashi UC, Greenwood K, Taylor DL, et al. **Poly(ADP ribose) polymerase cleavage precedes neuronal death in the hippocampus and cerebellum following injury to the developing rat forebrain.** *Eur J Neurosci* 1999;11:91–100
20. Tien RD and Ashdown BC. **Crossed Cerebellar Diaschisis and Crossed Cerebellar Atrophy: correlation of MR findings, clinical symptoms, and supratentorial diseases in 26 patients.** *AJR Am J Roentgenol* 1992;158:1155–1159
21. Lim JS, Ryu YH, Kim BM, Lee JD. **Crossed cerebellar diaschisis due to intracranial hematoma in basal ganglia or thalamus.** *J Nucl Med* 1998;39:2044–2047
22. Rutherford MA, Pennock JM, Dubowitz LMS, Cowan FM, Bydder GM. **Does the brain regenerate after perinatal infarction?** *Eur J Pediatr Neurol* 1997;1:13–18
23. Carr LJ. **Development and reorganization of descending motor pathways in children with hemiplegic cerebral palsy.** *Acta Paediatr Suppl* 1996;416:53–57
24. Rutherford MA, Pennock JM, Schwieso JE, Cowan FM, Dubowitz LMS. **Hypoxic-ischaemic encephalopathy: early and late magnetic resonance findings in relation to outcome.** *Arch Dis Child* 1996;75:145–151
25. Jouvet P, Cowan F, Cox P, et al. **Reproducibility and accuracy of magnetic resonance imaging studies of the brain after birth asphyxia.** *AJNR Am J Neuroradiol* 1999;20:1343–1348
26. Mercuri E, Ricci D, Cowan F, et al. **Head growth in infants with hypoxic-ischaemic encephalopathy: correlation with neonatal magnetic resonance imaging.** *Pediatrics* 2000;106:235–243
27. Press GA, Murakami J, Courchesne E, et al. **The cerebellum in sagittal plane: anatomic-MR correlation, 2: the cerebellar hemispheres.** *AJR Am J Roentgenol* 1989;153:837–846